JOURNAL OF SPACECRAFT AND ROCKETS
Vol. 37, No. 6, November–December 2000

Numerical Simulation of Transient Jet-Interaction Phenomenology in a Supersonic Freestream

Houshang B. Ebrahimi*
Sverdrup Technology, Inc., Arnold Air Force Base, Tennessee 37389

The objective is to evaluate the transient effects of a reaction control jet on the aerodynamic performance of a generic interceptor missile operating at supersonic flight conditions. Three-dimensional computations of the highly turbulent flowfield produced by a pulsed, supersonic, lateral-jet control thruster interacting with the supersonic freestream and missile boundary layer of a generic interceptor missile are evaluated at different altitudes and thruster conditions. A generic missile interceptor configuration consisting of a long, slender body containing fixed dorsal and tail fins is simulated. Parametric computational fluid dynamic solutions are obtained at altitude conditions corresponding to 19.7 and 35.1 km for 1) steady-state conditions with the lateral control jet turned off, 2) steady-state conditions with the lateral control jet turned on, 3) transient jet startup conditions, and 4) transient jet shutdown conditions. A thermally and calorically perfect gas with a specific heat ratio equal to 1.4 was assumed for both the Mach number 5 freestream and Mach number 3 lateral jet. Vehicle forces and moments are assessed from each solution by integrating the surface pressures and viscous shear stresses computed on the missile surfaces. These results are used to determine the influence of the jet-interaction effects on the transient aerodynamic performance of the missile. The analysis predicts strong transient influences for the integrated normal force and pitching moment.

Nomenclature

D	=	diameter of missile, m
L	=	length of missile, m
M	=	Mach number
P	=	static pressure, atm
P_{oj}	=	stagnation pressure, divert jet, Pa
T	=	static temperature, K
T_{oj}	=	stagnation temperature, divert jet, K
γ	=	ratio of specific heats

Introduction

TO complete its mission successfully, a missile defense interceptor must be highly maneuverable as it travels at supersonic or hypersonic speeds. Quick-response maneuverability, especially during the end-game phase of the interceptor's mission, is achieved by a rapid airframe response time to the attitude control system. Surface-mounted, fast-reacting, lateral-jet control thrusters issuing at large angles relative to the interceptor's direction of flight offer an effective supplement to conventional aerodynamic control surfaces, producing the required response times and improving the missile's agility and maneuverability.

The mutual interference of the control jet thruster exhaust with the supersonic freestream leads to thrust and moment amplifications due to high-pressure regions that form upstream of the jet on the missile surface. This high-pressure region is created by the shock structure that develops in the supersonic freestream in front of the lateral jet. Large regions of separated flow created by the missile boundary-layer interactions with the shock cause the high-pressure area to increase in size. This effect amplifies the response of the divert jets. Effective exploitation of this effect can lead to improved effectiveness of the missile interceptor. Insight into this phenomenon is necessary because at some missile orientations and flow conditions, the mutual interference of the jet-thruster flowfield with the freestream leads to deamplification, that is, negative effects. Therefore, an understanding of the controlling factors that produce thrust amplification, as well as those that produce thrust deamplification, is critical to developing a credible design basis for optimal missile aerodynamic performance. The jet-interaction (JI) phenomena are described more completely in Refs. 1 and 2.

The operation of a divert-jet control thruster is a time-dependent event. There is a ramp-up time interval in which the jet goes from quiescence to full thrust, followed by a relatively steady-time interval at full thrust, and then a jet-off time interval in which the jet thrust decays from full thrust back to quiescence. Typically this duty cycle lasts on the order of milliseconds, during which time the flowfield environment and, consequently, the interceptor missile responds to the jet in a time-dependent manner. Most computational fluid dynamics (CFD) predictions, however, assume a steady full-on jet and compute a corresponding steady-state solution, ignoring the transient events. Predictions from such analysis may not be completely adequate for control system design purposes or ground tests in which a complete jet duty cycle is included.

The CFD solutions completed for this investigation demonstrate the potential to numerically simulate complex, three-dimensional JI flowfields and assess the influence of the transient JI effects on the aerodynamic performance of the interceptor missile. However, just as JI phenomena pose a challenge for ground-test simulations, it is a formidable area for numerical simulations as well. There are very few documented experiments or numerical simulations performed to predict the transient effects of a pulsating divert jet on the force and moments of a supersonic missile. However, an experiment by Naumann et al.[3] shows that transient effects are important and must be considered in a complete JI evaluation. Numerically simulating the transient, lateral-jet control thruster flowfield behavior as it develops, merges, and interacts with the supersonic freestream flow over the missile body is one of the most complex propulsion flowfield phenomena to be addressed using state-of-the-art CFD techniques. A numerical scheme applied to simulate transient JI flowfield behavior must include the capability to accurately resolve the complex shock structures and boundary-layer separation regions associated with such flows, and also predict the time-accurate characteristics of these highly vortical and possibly chemically reacting flows. (The scope of this study does not include chemical effects.)

Reference 2 includes validation results of this CFD methodology for steady-state JI conditions through quantitative comparisons with ground-test measurements. These results produced reasonable agreements. However, resolved transient measurements from ground simulations are not available for validating CFD solutions.

The purpose of this paper is to 1) demonstrate the feasibility of CFD techniques to analyze JI flow transient behavior, 2) provide an extensive interrogation of computational flowfield results obtained

Received 10 August 1999; revision received 5 April 2000; accepted for publication 10 May 2000.

*Engineer Specialist, Arnold Engineering Development Center Group. Member AIAA.

at representative operational conditions, and 3) computationally visualize and quantify the transient JI effects resulting from a pulsed, lateral-jet control thruster on missile aerodynamic performance.

Approach

The approach consists of a computational experiment to numerically simulate JI flowfield behaviors, including evaluation of the resulting forces and moments, at two representative altitude conditions for a generic Mach number 5 interceptor missile and a Mach number 3 lateral control jet. The effects of the divert jet under transient startup and shutdown are evaluated, as are steady-state JI behaviors. Steady-state solutions of the supersonic flow surrounding the missile were also obtained with the divert thruster present, but not operating, on the missile body. The same missile and divert thruster geometries are assumed for all simulations. The generic missile geometry shown in Fig. 1 was provided by the Johns Hopkins University, Applied Physics Laboratory. A generic, long, slender missile body design, $L/D = 14.5$, including forward and aft fins, was evaluated. This geometry is representative of interceptor designs and was selected because divert-thruster transient effects are suspected to be influenced by the presence of fins on the missile. The missile freestream Mach number is maintained at 5.0. The Mach number at the exit of the diverging divert thruster's nozzle is nominally 3. A thermally and calorically perfect gas ($\gamma = 1.4$) was assumed in the CFD approximation for the freestream and the divert flow. Three-dimensional flowfield solutions were completed to assess the interceptor/divert-motor flowfield interactions at two altitude conditions, 19.7 km and 35.1 km. The angle of attack of the interceptor was specified as 0 deg. The divert jet was maintained at the same position on the interceptor missile with its nozzle axis situated at 90 deg to the thrust vector of the interceptor for all simulations.

The resulting CFD flowfield solutions are compared to determine the transient effects of divert-thruster jet startup and shutdown behaviors as functions of altitude. The flowfield surrounding the interceptor missile body with the divert thruster present, but not operating, on the interceptor body is also computed. Even when the divert jet is turned off, there is an influence on the missile body forces due to cavity flow created by the presence of the thruster opening on the body. This analysis was completed at two altitudes to determine the altitude effect, if any, on the interaction behavior and resulting missile body forces and moments.

The divert jet is located between two of the dorsal fins at the center of gravity for the interceptor missile. The divert-jet thrust chamber consisted of a converging/diverging nozzle geometry, and stagnation conditions were specified such that the nominal Mach number at the nozzle exit was 3.0. The divert-jet flow was included in the computational domain. The stagnation conditions specified for the divert thruster are $P_{oj} = 176$ atm and $T_{oj} = 2278$ K.

The freestream conditions for the two altitudes investigated are shown in Table 1.

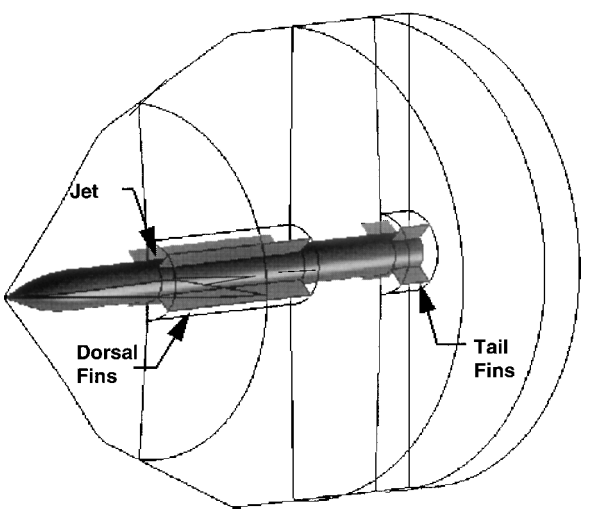

Fig. 1 Surface definition showing zonal decomposition.

Table 1 Supersonic interceptor missile freestream conditions

Parameter	Altitude = 19.7 km	Altitude = 35.1 km
Flight Mach number	5.0	5.0
Static pressure, atm	0.57	0.055
Air density, kg/m^3	0.0938	0.0082
Static temperature, K	216.67	237.2
Missile velocity, m/s	1475.0	1543.3
Angle of attack, deg	0.0	0.0
Yaw angle, deg	0.0	0.0
Molecular weight (air)	28.967	28.967
Ratio of specific heats	1.4	1.4

Table 2 JI CFD cases

Case number	Time integration	Jet flow	Mach number	Altitude, km
1	Steady state	Off	5	19.7
2	Steady state	On	5	19.7
3	Transient	Jet turning on	5	19.7
4	Transient	Jet turning off	5	19.7
5	Steady state	Off	5	35.1
6	Steady state	On	5	35.1
7	Transient	Jet turning on	5	35.1
8	Transient	Jet turning off	5	35.1

The CFD solutions were designed to study flowfield behaviors focusing on transient force and moment effects resulting from the operation of a Mach number 3.0 divert jet, located at the center of gravity on a Mach number 5 interceptor missile. The CFD flowfield simulates the interactions of the Mach number 3.0 divert jet as it discharges perpendicular to the Mach number 5 freestream flow. The CFD investigation included four solutions at each of the altitudes mentioned. The solutions comprised steady-state calculations with the divert thruster turned off and a steady-state solution with the jet on, as well as the transient startup of the jet and a transient shutdown of the jet. The eight CFD solution scenarios investigated are summarized in Table 2.

Geometry and Computational Grid

The generic interceptor missile geometry was specified as a relatively long and slender configuration ($L/D = 14.5$) equipped with fixed dorsal and tail fins. The divert-thruster nozzle exit was positioned flush with the missile surface between the dorsal fins at the center of gravity of the missile. The total length of the interceptor missile was specified as 4.97 m, which is equivalent to 14.5 calibers. One caliber is equivalent to one missile diameter, specified as 0.343 m. The nose geometry was modeled as a 2-caliber-long tangent ogive with a 0.0084-m-radius spherical nose cap. The afterbody section is a 12.5-caliber-long cylinder. Very thin dorsal and tail fins, rectangular in cross section, are symmetrically positioned around the body at 45 and 135 deg from the pitch plane. The dorsal fins have a 5-caliber chord and a 0.5-caliber span, with the leading edge located 5 calibers from the missile nose tip. The tail fins have a 1-caliber chord and a 0.5-caliber span with the leading edge located 13.5 calibers from the missile nose tip. The circular divert-jet thrust chamber exit is flush to the missile body at 90 deg to the thrust vector of the missile. The exit diameter is 0.0753 m. As shown in Fig. 1, the center of the divert-jet exit is located on the interceptor missile body 6 calibers from the missile nose tip (between the dorsal fins) in the vehicle pitch plane.

A computational grid was constructed for this geometry that includes the interceptor missile and the internal thrust chamber of the divert thruster. The grid consists of 13 blocked meshes (approximately 2.6 million grid points) for the low-altitude cases and 14 blocked meshes (approximately 3 million grid points) for the high-altitude cases. An additional mesh was required for the high-altitude cases to completely capture the relatively larger underexpanded jet plume that occurs at the higher altitude, lower ambient pressure environment. A convergent/divergent nozzle having supersonic exit conditions produces the jet thrust. The nominal exit Mach number of the divert jet is 3.0. An enlargement of the grid near the divert-jet location on the missile surface is shown in Fig. 2. A very high

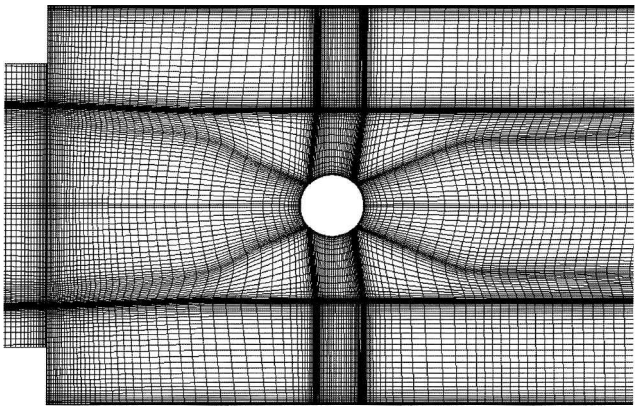

Fig. 2 Closeup view of surface grid around nozzle exit.

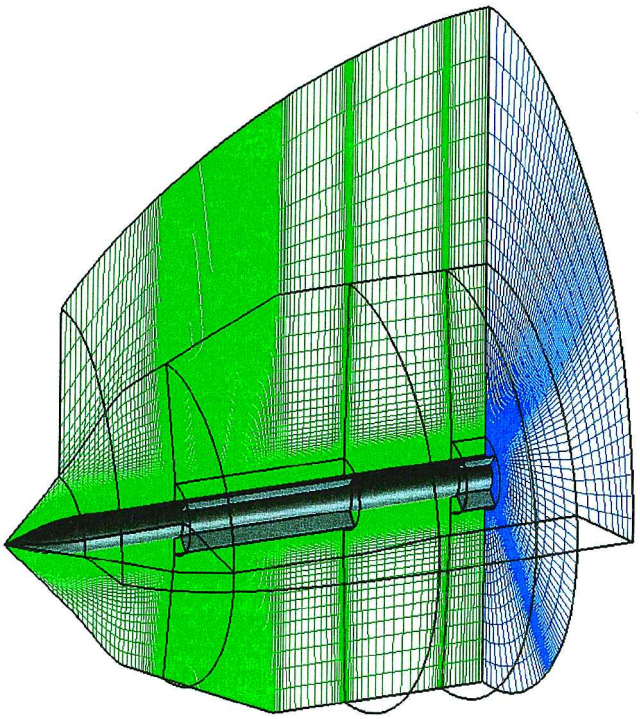

Fig. 3 Volume grid with high-altitude auxiliary grid.

grid density was constructed in the region upstream of the divert-jet exit to obtain spatial details of the flow gradients in this complex JI region. A pitch plane of symmetry was assumed for all cases. The volume grid for the freestream computational domain including all blocked meshes is shown in Fig. 3. Grid points were packed near solid walls to capture viscous effects. Grid sensitivity was not evaluated.

Analysis

The General Propulsion Analysis Chemical Kinetic and Two-Phase code, GPACT,[4] was applied exclusively to simulate the complex flowfields at each condition. GPACT solves the integral form of the three-dimensional, time-dependent, Reynolds-averaged, full, compressible Navier–Stokes equations. GPACT is capable of solving subsets of these equations, including two-dimensional and axisymmetric equations. GPACT includes an optional multizone capability, which was applied in this study. The algorithm employs a shock-capturing solution scheme. This methodology is fully conservative because of the consistent manner in which properties such as computational cell volumes, surface areas, and numerical-flux functions are evaluated. The flow solver contains thermodynamic models and chemistry models. High-temperature effects such as vibrational relaxation and preferential dissociation can be included in the calculations. For this investigation, a thermally and calorically perfect gas was assumed. Several turbulence models are provided as user-selected options. The turbulence models include the two-layer algebraic model of Baldwin and Lomax and fully coupled, two-equation k–ε models. An approximation accounting for turbulence–chemistry interactions is also available. The current study uses Van Leer flux splitting and a k–ε turbulence model. Forces and moments on the missile body were obtained by integrating the surface pressures and viscous shear stresses over the entire surface of the missile. The effect of the interceptor base entrainment and associated forces was not evaluated. Divert-jet thrust was obtained by integrating the calculated flux across the nozzle exit of the jet.

Results and Discussion

The GPACT model provided converged flowfield solutions for all cases considered in the numerical investigation. For the steady-state solutions, CFD convergence was determined by five orders of magnitude reduction in the computed residuals and constant flowfield behavior. Computational times for converged steady-state solutions required 50 (CPU) h on a high-performance computer using eight processors. Lesser CPU time was required for solutions obtained when the divert thruster was not operating. The transient computations were executed in a time-accurate mode and required considerably longer CPU times. Additionally, transient CFD analyses cannot take advantage of convergence acceleration techniques. The transient computations required 20–40 CPU h to integrate over 1 ms of physical time, depending on the Courant–Friedrichs–Lewy number and the grid resolution. Initially, a time step of 0.2 μs was used for the transient solutions. This value was increased in a stepwise fashion to 0.5 μs as the computation proceeded. To ensure an eventual steady-state condition, the transient methodology was continued to 14 ms.

Freestream conditions were specified on the far-field boundaries, and viscous no-slip assumptions were specified on all missile surfaces, including the divert-jet thruster chamber walls. The thrust chamber boundary conditions specified for the divert-nozzle inflow depended on whether the thruster jet was operational. In the jet-off case, the nozzle inflow boundary is replaced with a slip wall; otherwise, a subsonic inflow boundary condition is used for the jet-on simulations. The divert-thruster stagnation conditions $P_{oj} = 176$ atm and $T_{oj} = 2278$ K were specified for the jet subsonic inflow boundary condition. Outflow boundary conditions equal to the freestream ambient conditions were specified for the missile downstream boundary. For those simulations where the divert jet was turned off, the empty thrust chamber cavity, embedded within the interceptor surface, is included in the computational domain. Because the interceptor missile base aerodynamic effects were not computed, the force and moment contributions of the base region were neglected.

Flowfield results for the 19.7-km altitude steady-state, jet-on calculation are shown in Fig. 4. Mach number contours at three axial

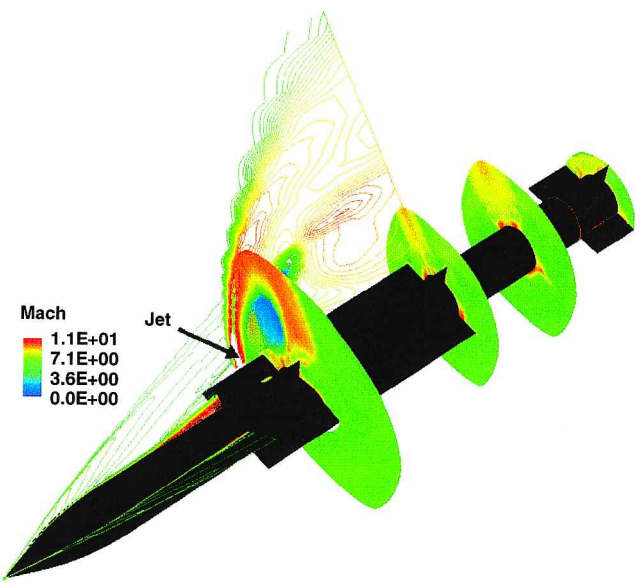

Fig. 4 Mach number contours for 19.7-km-altitude, jet-on case.

locations on the missile body are presented: 1) just downstream of the divert jet, 2) at the end of the dorsal fins, and 3) at the end of the missile. The behavior of the underexpanded divert jet is indicated by the rapid divergence of the jet exhaust in the first cross section. Effects of the divert-jet and freestream interactions are noticeable at the downstream locations. Note the high-pressure, that is, low-Mach-number, interaction region impinging on the fins in cross section 2.

Because the divert jet operates in an underexpanded mode at both altitude conditions, the flow at the nozzle exit plane is supersonic (approximately Mach number 3.0). At these conditions, the internal thrust chamber flowfield conditions are independent of the freestream, resulting in identical steady-state internal thrust chamber flowfields at both altitudes. However, the divert-jet thrust at the higher altitude is expected to be larger because of the smaller ambient force at the nozzle exit. Computed velocity vectors resulting from the jet-on steady-state solution, including the divert-jet thrust chamber and immediate freestream interaction region for the lower-altitude (19.7 km) Mach number 5 conditions, are shown in Fig. 5. The large circulation bubble created by the freestream interaction with the divert-jet plume is evident in the region upstream of the divert nozzle exit. The formation of a secondary separation region is also apparent. These recirculation zones create a high-pressure region and an associated force on the missile surface. The force exerted by the recirculation modifies the divert jet's thrust force and influences the moment about the center of gravity of the interceptor missile. As indicated in Fig. 5, a separation region on the upstream side of the divert jet is evident. A separation region is also present on the downstream side, creating an expansion region.

Steady-state velocity vectors for the jet-on calculation, showing the divert-jet thrust chamber and immediate freestream flow region at 35.1 km, are presented in Fig. 6. The same divert-jet thrust chamber conditions used for the lower-altitude simulation were also used for this higher-altitude condition; therefore, the divert-jet nozzle is even more underexpanded at the higher altitude. The underexpansion nozzle condition results in a larger exhaust plume expansion angle and deeper jet penetration into the freestream flow regions

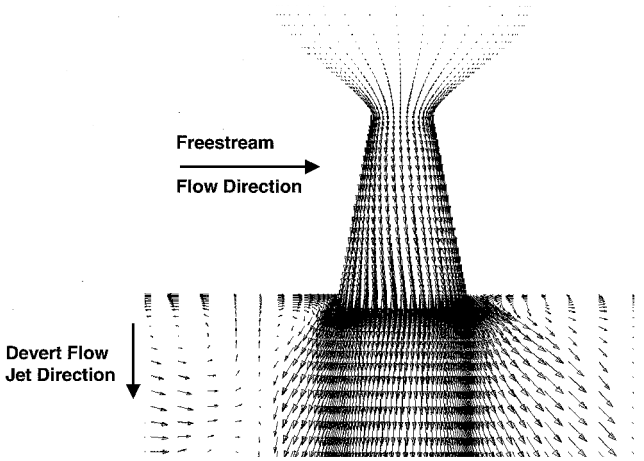

Fig. 5 Velocity vectors for 19.7-km-altitude, jet-on case.

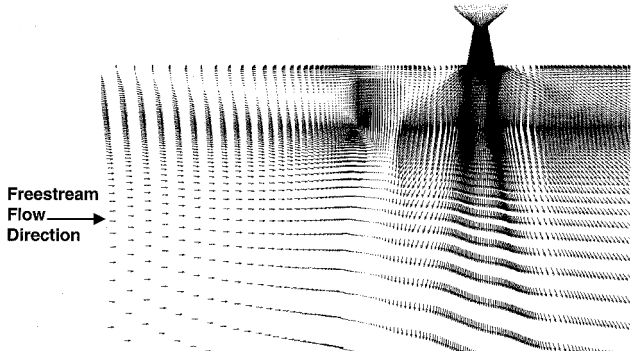

Fig. 6 Velocity vectors for 35.1-km-altitude, jet-on case.

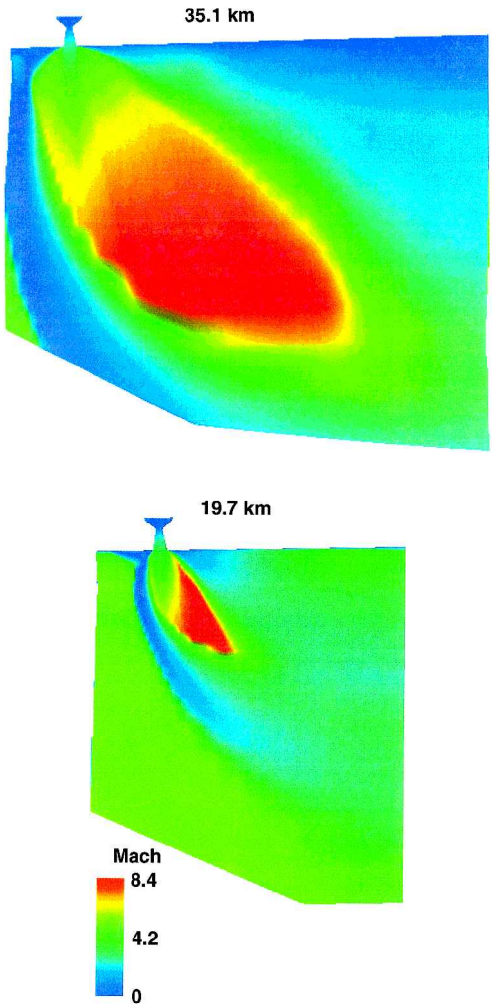

Fig. 7 Jet interaction Mach number contours: comparison of 19.7 and 35.1 km; $M = 5.0$.

when compared to the lower-altitude (19.7 km) results shown in Fig. 5. The higher-altitude case exhibits a much larger separation region because of the reduced momentum of the freestream, providing conditions that are more favorable for separation. Figure 7 shows a comparison of the steady-state Mach number contours for the 19.7- and 35.1-km solutions with the divert jet turned on. The lower ambient pressure at the high-altitude condition results in a significantly larger jet plume and separation region compared to the lower-altitude results. The effects on the upstream separation region and downstream expansion regions are also evident.

Figures 8–11 are the computed results of the transient JI solution at the 19.7- and 35.1-km-altitude conditions showing the effects of the divert jet startup process. Several transient time slices are shown, culminating in steady-state flow. Figures 8 and 9 depict the transient time slices of calculated static-pressure contours on the surface of the interceptor vehicle from initiation of the divert-jet flow, at $t = 0.0$, to established steady-state flow after approximately 6 ms. Note the high-pressure interaction region impinging on the dorsal fins at 3.5 ms for the low-altitude case (Fig. 8). Compared to the 19.7-km results, the plume is bigger at the higher-altitude condition, and the JI region impinges on the dorsal fins earlier, shown here at 3 ms (Fig. 9). However, because of the lower-pressure environment at 35.1 km, it is expected that the corresponding impingement force will be lower compared to the 19.7-km results. Consequences of this impingement will be observed in subsequent force analysis.

Mach number contours in the pitch plane of the missile over the same time span are shown in Figs. 10 and 11. These results clearly show the development of the jet shock and the associated high surface pressures and low Mach numbers in the recirculation zone upstream of the divert-jet exit location. The downstream expansion

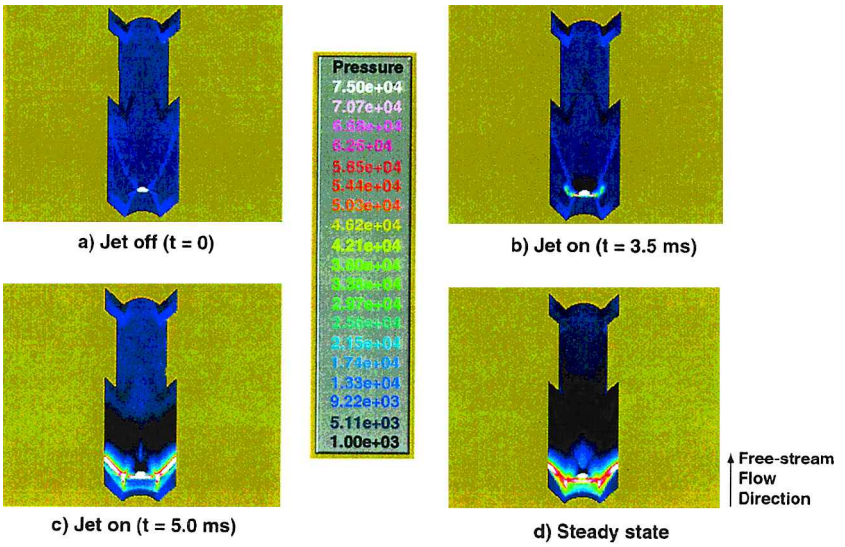

Fig. 8 Surface pressure at 19.7-km-altitude, jet startup transient process.

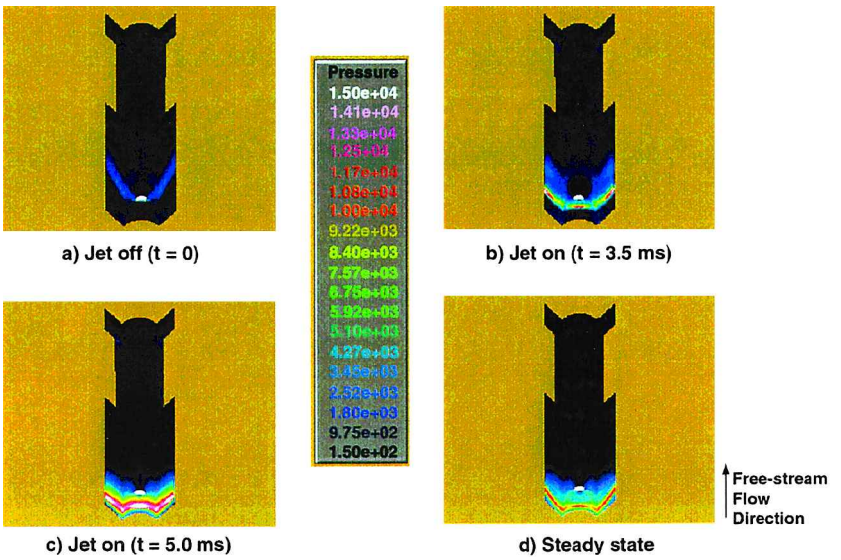

Fig. 9 Surface pressure for 35.1-km-altitude, jet startup transient process.

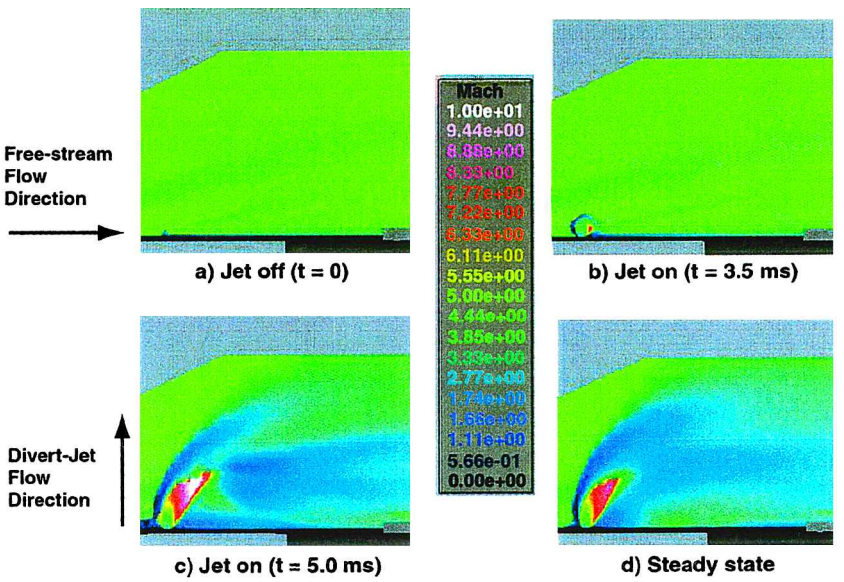

Fig. 10 Mach number contours for 19.7-km-altitude, jet startup transient process.

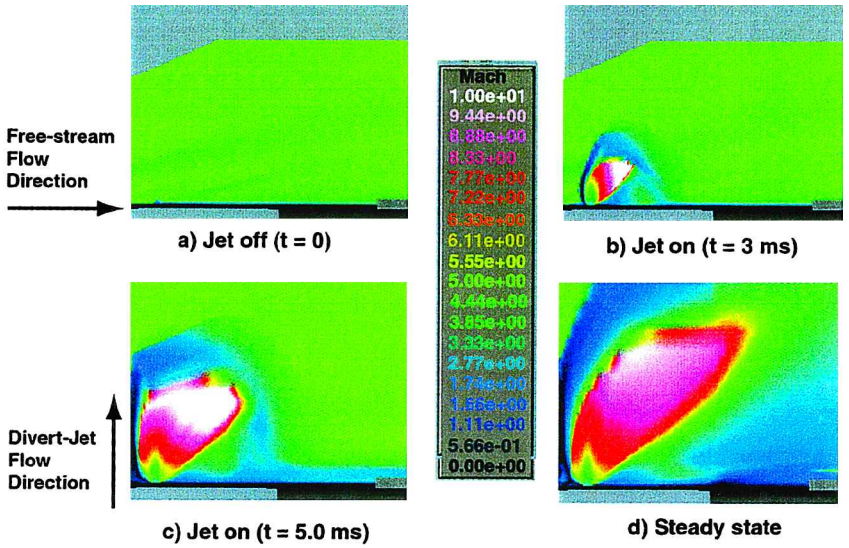

Fig. 11 Mach number contours for 35.1-km-altitude, jet startup transient process.

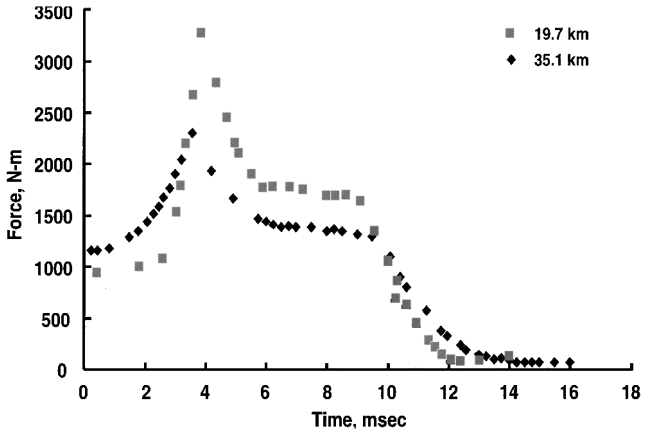

Fig. 12 Integrated normal force from start to shutdown at 19.7 and 35.1 km.

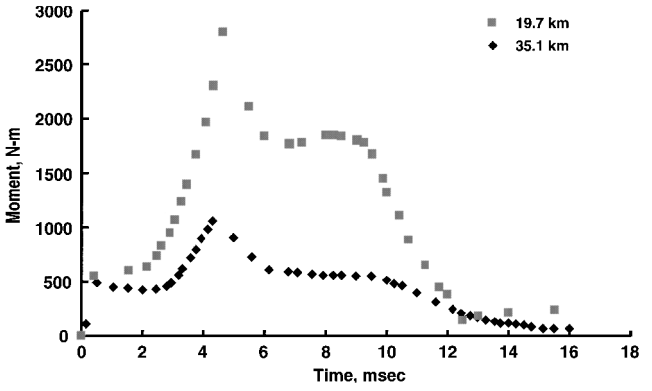

Fig. 13 Integrated pitching moment from start to shutdown at 19.7 and 35.1 km.

regions are characterized by supersonic flow and decreasing pressure. Evident in the high-altitude results are larger plume expansion, deep divert-jet penetration into the freestream, and very large recirculation regions. A small disturbance at the divert-jet location is apparent at $t = 0.0$ in Figs. 8–11. This feature results from the presence of the nozzle cavity before the initialization of the divert-jet flow.

To highlight the similarities and differences, the normal force and pitching moment over a complete divert-jet cycle spanning the transient jet startup, steady-state, and transient shutdown process are presented in Figs. 12 and 13. As shown in Fig. 12, at time = 0 ms, the jet is turned on and the force rises abruptly, reaching a value of approximately 920 N for the low-altitude condition and 1100 N for the high-altitude condition. This force is due to the jet thrust alone. Recall that the divert-jet thrust at the higher altitude is expected to be larger because of the smaller ambient force term at the nozzle exit. In both cases, the force continues to rise as a high-pressure recirculation region develops, covering increasing areas on the cylindrical missile body. Note that although the separation region is larger at the higher-altitude condition, the resulting pressure increase on the missile body is lower when compared to the lower-altitude case because of the smaller ambient pressure, which results in a decreased force at higher altitudes.

The enhanced transient effect begins at approximately 2.6 ms and creates a body normal force in excess of 3300 N after 3.8 ms for the lower-altitude condition. A steady-state condition is established after 6 ms. The steady-state force is approximately 1750 N and is greater than the magnitude of the jet force alone (920 N). As seen in Fig. 13, the pitching moment (computed about the center of the divert jet) quickly rises to a value of 550 N-m as the jet is turned on; it then appears to remain steady over the period from 0 to 2.8 ms. The pitching moment then rises to a value approaching 2800 N-m after 4.5 ms. Recall that the JI region impinges on the dorsal fins of the missile after 4 ms (Fig. 8). The effect of this impingement is evident in Figs. 12 and 13. Although the normal force reaches a maximum after 3.8 ms, the pitching moment continues to rise for another 0.7 ms. This delay in the maximum value of pitching moment is attributed to the impingement of the JI region on the dorsal fins, that is, there is a further change in moment with little change in force. After 4.0 ms, the high-pressure region established in front of the divert jet continues to travel upstream, causing a slight drop in surface pressure and pitching moment, as the moving shocks begin to settle down and become more stationary and oblique to the oncoming freestream flow. Although a net decrease in the normal force and pitching moment results from the separation region acting on the missile, the resulting steady-state force (1750 N) is almost double the force value computed for the divert jet alone (920 N). The resulting steady-state pitching moment (1800 N-m) is a factor of three greater than the pitching-moment value computed for the divert jet alone (550 N-m).

The high-altitude force and pitching-moment trends are similar when compared to the lower-altitude results, but are less abrupt. The transient spike occurs earlier in the startup process (3.5 vs 3.8 ms) and is more gradual compared with the lower-altitude solution. The JI impingement on the dorsal fins occurs earlier at the high-altitude, low-pressure condition (3 ms; Fig. 9); therefore, the delay in the maximum value of the pitching moment is predicted to be longer (1 vs 0.7 ms). Recall that the delay in the maximum value of pitching moment was correlated with the impingement of the JI region

on the missile dorsal fins. The peak transient interaction force (approximately 2200 N) at the higher-altitude condition is considerably less than the lower-altitude peak force (3300 N). This difference is attributed to the lower ambient pressures at the higher altitude.

After the jet is shutdown, the force and moment begin to decrease. The normal force appears to remain steady for approximately 1.1 ms at the lower altitude as the flowfield adjusts to the new condition. The moment, shown in Fig. 13, also appears to experience a delayed response to the jet shutdown and begins to decrease after a period of approximately 1.5 ms. The final jet-off steady-state force is equal to approximately 80 N, and the moment is equal to 120 N-m. Recall that the jet-off flowfield is not axisymmetric because of the jet cavity. The shutdown process requires approximately 4.5 ms to achieve steady-state conditions.

Corresponding results for the transient high-altitude solutions at 35.1 km are also shown in Figs. 12 and 13. These results are very similar to the shutdown behavior at the lower-altitude condition. The steady-state values at the end of the shutdown transient are lower because of the lower pressure in the freestream at the higher altitude. These results indicate that longer times are required to reach steady-state conditions at the high-altitude condition. Steady-state conditions were realized after approximately 6.0 ms, after the jet was shut down, compared to 4.5 ms for the lower-altitude condition. The very large jet-penetration and recirculation regions resulting at the higher altitude are assumed to contribute to the delay.

CFD results, such as these, can be used to more completely assess the interceptor missile reaction times and aerodynamic influences afforded by the operation of the divert motor. These results also indicate that CFD techniques can be applied to optimize the geometry configurations of integrated divert-motor missile-interceptor design features. CFD can be applied to gain insight into the JI region, including the enhancement effect of the JI separation region. Accounting for these effects can be used to ensure stable missile aerodynamics. Furthermore, these calculations strongly suggest that the transient effects predicted when the JI separation region impinges on the missile dorsal fin could have an influence on the aerodynamic behavior of the missile if they are not considered in the design analysis.

Summary

Jet-interaction computations were completed to assess the transient and steady-state effects of a supersonic divert-control thruster on the flowfield and aerodynamics resulting from a generic missile interceptor operating at supersonic flight conditions. The analyses include evaluation of flowfield phenomena, as well as predicted surface pressures, normal forces, and pitching moments on a generic interceptor missile at altitude conditions corresponding to 19.7 and 35.1 km. The results indicate a strong transient effect that must be considered when designing control algorithms for pulsed-jet reaction control systems with short pulse times. The transient interactions at lower altitudes on this type of finned interceptor missile geometry resulted in short durations of very high forces that appear to diminish at higher altitudes. These forces appear to be enhanced by the impingement of the high-pressure separation region that forms in front of the divert jet on the dorsal fins of the interceptor missile. These pressures are higher than the steady-state pressure values because of the moving shock resulting from the JI phenomena. The duration of the transient effects is predicted to be approximately 3–4 ms at both high and low altitudes before the force begins to decrease and approach steady-state values. The transient results indicate that the divert-jet shutdown process requires more time to reach steady-state conditions when compared with the jet startup process.

This investigation demonstrates the utility of state-of-the-art CFD tools to address issues pertaining to one of the most complex flow interactions of interest in the propulsion arena today. Although these solutions required considerable CPU resources, they provide an economical means to supplement the costly interceptor design and testing process and, therefore, have the potential to save development and testing resources. CFD solutions can be applied to optimize the test condition matrices and to evaluate candidate missile/divert-jet geometries and operating conditions to identify potential problem areas before production. The CFD flowfields can be analyzed to gain insight into the force amplification phenomena and to understand and properly account for the transient behavior. The flowfield details calculated and visualized in this study cannot be measured in the harsh testing environments using modern flow visualization and measurement techniques. Additional CFD studies investigating the effects of chemistry in the interaction region are needed to complete the CFD feasibility demonstration.

Acknowledgments

The author would like to recognize the contributions of Martha Simmons and R. L. Spinetti for reviewing the technical aspects of this study and editing the manuscript.

References

[1] Srivastava, B., "Lateral Jet Control of a Supersonic Missile: CFD Predictions and Comparison to Force and Moment Measurements," AIAA Paper 97-0639, Jan. 1997.

[2] Ebrahimi, H. B., "Validation Database for Propulsion Computational Fluid Dynamics," *Journal of Spacecraft and Rockets*, Vol. 34, No. 5, 1997, pp. 642–650.

[3] Naumann, K. W., Ende, H., George, A., and Mathieu, G., "Stationary and Time-Dependent Effect in Near Interaction of Gaseous Jets and Supersonic Cross Flow," AIAA Paper 98-2972, Jan. 1998.

[4] Ebrahimi, H. B., and Kawasaki, A., "Numerical Investigation of Exhaust Plume Radiative Transfer Phenomena," AIAA Paper 98-3623, July 1998.

R. M. Cummings
Associate Editor

Color reproductions courtesy of Arnold Engineering Development Center.